American Mineralogist, Volume 71, pages 727–733, 1986

Low albite, $NaAlSi_3O_8$: Neutron diffraction study of crystal structure at 13 K

JOSEPH V. SMITH, GILBERTO ARTIOLI
Department of Geophysical Sciences, University of Chicago, Chicago, Illinois 60637
ÅKE KVICK
Chemistry Department, Brookhaven National Laboratory, Upton, New York 11973

ABSTRACT

The crystal structure of low albite, Amelia, Virginia, was determined at 13 K by neutron diffraction (a = 8.1151(8), b = 12.7621(25), c = 7.1576(6) Å, α = 94.218(12)°, β = 116.803(8)°, γ = 87.707(13)°; $C\bar{1}$). Mean T–O distances are T_1O 1.743, T_1m 1.611, T_2O 1.615, T_2m 1.616 Å. Refinement of scattering lengths yields the following populations: T_1O 0.997(4) Al; T_1m 1.001(3) Si; T_2O 1.002(3) Si; T_2m 1.006(4) Si; Na 0.972(1) Na. The displacement of the Na atom is represented by an ellipsoid (root-mean-square amplitudes 0.065, 0.073, and 0.108 Å) whose shorter axes are constrained by the five near oxygen atoms at 2.361, 2.419, 2.438, 2.500, and 2.614 Å. The displacements of all atoms (B_{iso}: Si 0.19, Al 0.20, O 0.29–0.42, Na 0.56 Å^2) are similar to those for natrolite and scolecite at 20 K and are consistent with qualitative expectations for the zero-point energy. Stereochemical interpretation of the T–O distances at low temperature in low albite, natrolite, scolecite, quartz, and cristobalite is incomplete when only first neighbors are considered.

INTRODUCTION

It is difficult to explain the geometrical properties of framework structures in terms of theories of chemical bonding. Qualitative and quantitative studies of small atomic clusters provide a useful first approximation (reviewed by Gibbs, 1982), but further progress will require lattice summations based on appropriate algorithms. Simple electrostatic models (reviewed by Catlow and Mackrodt, 1982) are inadequate for framework structures, and a bond-bending term is needed to simulate molecular-orbital contributions. Most of the present diffraction data on crystal structures of frameworks are inappropriate as a test of bonding models because measurements were made at elevated temperature. Thermal energy may cause major changes in framework geometry (e.g., the Si–O–Si angle in low cristobalite changes from 144.7(1)° at 10 K to 148.5(1)° at 293 K; Pluth et al., 1985). Furthermore, thermal vibration produces apparent bond shortening because the distances are calculated between the centroids of electron density or neutron scattering profiles (Busing and Levy, 1964). This also gives biased values for the bond angles. The present study of low albite is part of a systematic program to generate accurate data at low temperature for important framework structures including silica polymorphs (quartz, Lager et al., 1982; cristobalite, Pluth et al., 1985) and zeolites (natrolite, Artioli et al., 1984; scolecite, Kvick et al., 1985).

Harlow and Brown (1980) determined the crystal structure of a low albite from Amelia, Virginia, using both neutron and X-ray diffraction studies at ambient temperature. Mechanical failure of a cryostat aborted a follow-up study at low temperature, and we are indebted to Harlow and Brown for the generous loan of their crystal for the present study. Winter et al. (1977) determined the structure of a low albite from Tiburon, California, at 773, 1023, and 1243 K, using X-ray methods; however, we were unable to find a good single crystal of Tiburon albite large enough for neutron diffraction. Together with other structure analyses (Ferguson et al., 1958; Prewitt et al., 1976; Quareni and Taylor, 1971; Ribbe et al., 1969; Wainwright in Smith, 1974; Wenk and Kroll, 1984; Winter et al., 1979), these studies provide a thorough description of the structural features of low and high albites from room temperature to the melting point. Pioneering structure analyses of high and low albite at 93 K (Williams and Megaw, 1964) were important indicators of low-temperature effects.

EXPERIMENTAL TECHNIQUE

The crystal provided by Harlow and Brown weighs 0.0264 g and has a volume of 10 mm^3. A temperature of 13 K was attained with a DISPLEX CS-202 refrigerator (Air Products and Chemicals, Inc.). A monochromatic neutron beam from the Brookhaven National Laboratory High Flux Beam Reactor was obtained by reflection from the (002) plane of a Be crystal. The wavelength 1.0505(1) Å was determined by least-squares fit of 61 $\sin^2\theta$ values from a KBr crystal (a_0 = 6.6000(1) Å at 298 K). Cell parameters for low albite at 13 K determined from 60 $\sin^2\theta$ values (44° < 2θ < 57°) are a = 8.1151(8); b = 12.7621(25); c = 7.1576(6) Å; α = 94.218(12)°; β = 116.803(8)°; γ = 87.707(13)°. A total of 2804 reflections ($\pm h + k \pm l$) was collected out to $\sin\theta/\lambda$ = 0.784 Å^{-1} using $\theta - 2\theta$ step scans with scan width $\Delta 2\theta$ = 3.0° (2θ < 60°) and 1.5(1 + 2.0 tan θ)° for 60° < 2θ < 114°. The data were cor-

0003–004X/86/0506–0727$02.00

Table 1. Atomic parameters for room temperature (Harlow and Brown, 1980) and 13 K (this paper)

Site		Occupancy		x	y	z	B_{eq}
T_1O	RT	0.970(20)	Al	901(10)	16862(6)	20806(11)	0.60(1)
	13	0.997(4)	Al	896(5)	16774(3)	20773(6)	0.20(1)
T_1m	RT	0.965(20)	Si	386(8)	82062(5)	23728(9)	0.51(1)
	13	1.001(3)	Si	359(4)	82131(3)	23701(5)	0.19(1)
T_2O	RT	1.0	Si	69209(8)	11306(5)	31508(9)	0.54(1)
	13	1.002(3)	Si	69041(4)	10996(3)	31323(5)	0.19(1)
T_2m	RT	1.0	Si	68152(8)	88195(5)	36078(9)	0.53(1)
	13	1.006(4)	Si	67890(4)	88190(3)	35960(5)	0.20(1)
Na	RT	0.986	Na	26849(13)	98870(10)	14672(18)	2.66(2)
	13	0.972(1)	Na	26470(6)	98952(1)	14441(7)	0.56(1)
O_{A1}	RT	1.0	O	490(7)	13115(4)	96638(7)	0.95(1)
	13	1.0	O	565(3)	12907(2)	96644(4)	0.34(1)
O_{A2}	RT	1.0	O	59229(6)	99755(4)	28053(7)	0.72(1)
	13	1.0	O	58864(3)	99755(2)	27889(4)	0.29(1)
O_BO	RT	1.0	O	81231(7)	11013(4)	19056(8)	1.04(1)
	13	1.0	O	81264(3)	10794(2)	19019(4)	0.36(1)
O_Bm	RT	1.0	O	82027(7)	85114(4)	25876(9)	1.32(1)
	13	1.0	O	81931(3)	85141(2)	25924(4)	0.42(1)
O_CO	RT	1.0	O	1342(6)	30252(4)	27026(8)	0.92(1)
	13	1.0	O	1020(3)	30192(2)	26814(4)	0.34(1)
O_Cm	RT	1.0	O	2398(7)	69389(4)	22991(8)	0.94(1)
	13	1.0	O	2294(3)	69437(2)	22592(1)	0.34(1)
O_DO	RT	1.0	O	20770(7)	10901(4)	38910(7)	1.02(1)
	13	1.0	O	21013(3)	10901(2)	38942(4)	0.36(1)
O_Dm	RT	1.0	O	18364(7)	86819(4)	43609(8)	1.15(1)
	13	1.0	O	18503(3)	86821(2)	43708(4)	0.38(1)

Estimated standard error in parenthesis refers to last digit.
Positional parameter multiplied by 10^5.

Table 2. Apparent thermal parameters: root-mean square amplitude (Å)

Site		B Equiv.	Axis 1	Axis 2	Axis 3
T_1O	RT	0.60(1)	0.0759(20)	0.0851(18)	0.0988(17)
	13K	0.20(1)	0.0444(20)	0.0492(17)	0.0576(16)
T_1m	RT	0.51(1)	0.0711(17)	0.0803(15)	0.0891(15)
	13K	0.19(1)	0.0426(17)	0.0469(15)	0.0561(14)
T_2O	RT	0.53(11)	0.0742(17)	0.0847(17)	0.0894(15)
	13K	0.19(1)	0.0461(15)	0.0463(16)	0.0543(14)
T_2m	RT	0.53(1)	0.0768(15)	0.0792(16)	0.0898(15)
	13K	0.20(1)	0.0465(16)	0.0483(15)	0.0571(14)
Na	RT	2.66(2)	0.1221(16)	0.1311(15)	0.2628(15)
	13K	0.56(1)	0.0650(14)	0.0728(13)	0.1078(10)
O_{A1}	RT	0.95(1)	0.0739(13)	0.1149(5)	0.1314(8)
	13K	0.34(1)	0.0454(9)	0.0727(6)	0.0741(6)
O_{A2}	RT	0.72(1)	0.0775(12)	0.0915(10)	0.1139(9)
	13K	0.29(1)	0.0524(9)	0.0578(7)	0.0705(6)
O_BO	RT	1.04(1)	0.0791(13)	0.1162(9)	0.1405(8)
	13K	0.36(1)	0.0482(9)	0.0724(6)	0.0794(6)
O_Bm	RT	1.32(1)	0.0787(13)	0.1410(9)	0.1551(8)
	13K	0.42(1)	0.0489(9)	0.0802(6)	0.0842(6)
O_CO	RT	0.92(1)	0.0805(12)	0.1102(10)	0.1276(9)
	13K	0.34(1)	0.0531(8)	0.0677(7)	0.0740(6)
O_Cm	RT	0.94(1)	0.0823(12)	0.1087(10)	0.1302(9)
	13K	0.34(1)	0.0523(9)	0.0672(7)	0.0750(6)
O_DO	RT	1.02(1)	0.0868(12)	0.1180(9)	0.1316(9)
	13K	0.36(1)	0.0502(8)	0.0722(7)	0.0779(6)
O_Dm	RT	1.15(1)	0.0845(12)	0.1228(9)	0.1470(9)
	13K	0.38(1)	0.0480(9)	0.0746(7)	0.0813(6)

rected for background using the first and last one-tenth of the scan. The maximum intensity variation from the mean of the standards 535 and 733 is 4%. Averaging yielded 2686 unique intensities with $R_w = 0.005$ for equivalent intensities. The absorption correction for a $6 \times 6 \times 6$ grid with calculated $\mu = 0.0041$ cm^{-1} yielded transmission factors of 0.9988–0.9993.

Refinement was straightforward using the technical procedures listed in Artioli et al. (1984), and starting parameters were those of Harlow and Brown (1980) (Tables 1–3). The number of reflections above 3σ is 2662, and the 129 parameters refined by least-squares minimization consist of three positional coordinates (Table 1) and six anisotropic displacement parameters for each of 13 atoms (Table 3), one scale factor, six anisotropic extinction coefficients (type I, Lorentzian mosaicity, Becker and Coppens, 1974), and five occupancy factors for the T and Na sites (Table 1).

Neutron scattering lengths were taken from Koester et al. (1981), and the occupancies of the four T sites indicate essentially complete segregation of Al into T_1O (0.997(4)) and full occupancy of the other sites by Si. Satisfactory refinement was obtained with one anisotropic Na site (Table 2), but the population factor of 0.972(1) is lower than the value of unity expected for charge balance with the $AlSi_3$ composition inferred from the population factors for the T sites. K has almost the same neutron scattering length as Na, and the small amounts of K and Ca in the electron-probe and chemical analyses listed by Harlow and Brown (1980) should not affect the occupancy factor of the Na site. Furthermore, the larger scattering lengths of K and Ca would increase the occupancy factor of the Na site. All attempted explanations of the low population factor for the Na site lack firm supportive evidence, and detailed discussion is unwarranted here. Reduction of the neutron scattering length of Na by 2–3% is an obvious possibility that is not inconsistent with the occupancy of 0.986(8) observed for Na in the refinement of natrolite at 20 K (Artioli et al., 1984).

Table 3. Apparent thermal vibration parameters

Site		B	β_{11}*	β_{22}	β_{33}	β_{12}	β_{13}	β_{23}
T_1O	RT	0.60(4)	326(12)	98(4)	314(15)	-29(5)	163(11)	10(6)
	13K	0.20(1)	98(7)	36(2)	109(8)	-9(2)	49(5)	8(3)
T_1m	RT	0.60(3)	266(9)	87(3)	278(12)	15(4)	147(9)	14(5)
	13K	0.19(1)	84(5)	38(2)	94(7)	3(2)	43(4)	10(2)
T_2O	RT	0.61(3)	259(10)	73(3)	381(13)	-12(4)	143(9)	19(5)
	13K	0.19(1)	80(5)	33(2)	113(7)	-1(2)	40(4)	11(2)
T_2m	RT	0.64(3)	228(9)	79(3)	380(13)	5(4)	138(9)	25(5)
	13K	0.20(1)	87(5)	38(2)	112(7)	0(2)	43(4)	12(2)
Na	RT	2.51(6)	580(15)	591(8)	1548(25)	-100(9)	400(15)	-515(1)
	13K	0.56(1)	162(7)	118(3)	320(9)	-12(3)	99(5)	-53(3)
O_{A1}	RT	0.98(3)	641(8)	159(3)	368(10)	-11(4)	304(7)	37(4)
	13K	0.34(1)	203(3)	63(1)	138(4)	-2(2)	97(3)	23(2)
O_{A2}	RT	0.76(3)	311(7)	78(2)	581(10)	-5(3)	165(7)	43(4)
	13K	0.29(1)	125(3)	39(1)	209(4)	-5(2)	59(3)	20(2)
O_BO	RT	1.10(3)	461(8)	174(3)	805(11)	-92(4)	419(8)	-29(4)
	13K	0.36(1)	157(3)	70(1)	254(4)	-23(2)	134(3)	4(2)
O_Bm	RT	1.33(3)	542(8)	233(3)	1076(12)	89(4)	582(8)	40(5)
	13K	0.42(1)	160(3)	81(1)	313(4)	18(2)	161(3)	13(2)
O_CO	RT	0.97(3)	404(8)	98(2)	754(11)	-57(3)	237(8)	-20(4)
	13K	0.34(1)	139(3)	46(1)	255(4)	-19(2)	79(3)	-2(2)
O_Cm	RT	1.00(3)	421(8)	92(2)	701(10)	39(3)	167(7)	33(4)
	13K	0.34(1)	147(3)	43(1)	235(4)	18(2)	59(3)	18(2)
O_DO	RT	1.04(3)	476(8)	175(3)	409(10)	39(4)	84(7)	44(4)
	13K	0.36(1)	158(3)	71(1)	138(4)	12(2)	30(3)	20(2)
O_Dm	RT	1.18(3)	542(8)	180(3)	431(10)	-55(4)	12(7)	-15(4)
	13K	0.38(1)	157(3)	72(1)	138(4)	-20(2)	8(3)	-3(2)

β multiplied by 10^5. Estimated standard error in parentheses refers to last digit. B is B_{iso} for RT and B_{eq} for 13 K.
*The anisotropic temperature factor is defined as $\exp(-(h^2.\beta_{11} + \ldots 2hk.\beta_{12} + \ldots)$.

Table 4. T–O and tetrahedral O–O bond distances

T_1O-O	RT	13K	T_1m-O	RT	13K
A1	1.7472(9)	1.7495(5)	A1	1.5955(8)	1.6002(4)
BO	1.7446(10)	1.7433(5)	Bm	1.6000(9)	1.6027(4)
CO	1.7348(9)	1.7344(5)	Cm	1.6214(8)	1.6208(5)
DO	1.7448(10)	1.7461(5)	Dm	1.6179(8)	1.6186(5)
Average	1.7429	1.7433	Average	1.6087	1.6106
T_2O-O	RT	13K	T_2m-O	RT	13K
A2	1.6322(8)	1.6311(4)	A2	1.6448(8)	1.6450(5)
BO	1.5918(8)	1.5946(4)	Bm	1.6205(8)	1.6209(4)
Cm	1.6171(8)	1.6168(5)	CO	1.5957(8)	1.5968(5)
Dm	1.6152(8)	1.6166(4)	DO	1.6015(8)	1.6032(4)
Average	1.6141	1.6148	Average	1.6156	1.6165
T_1O	RT	13K	T_1m	RT	13K
A1-BO	2.7310(9)	2.7296(4)	A1-Bm	2.6010(9)	2.6164(4)
CO	2.9528(10)	2.9605(6)	Cm	2.6747(8)	2.6744(6)
DO	2.7525(8)	2.7449(5)	Dm	2.5883(8)	2.5918(4)
BO-CO	2.8881(8)	2.8842(6)	Bm-Cm	2.6100(8)	2.6123(5)
DO	2.8783(10)	2.8794(5)	Dm	2.6570(10)	2.6605(5)
CO-DO	2.8518(8)	2.8586(7)	Cm-Dm	2.6210(8)	2.6237(6)
T_2O	RT	13K	T_2m	RT	13K
A2-BO	2.6595(9)	2.6588(5)	A2-Bm	2.6258(8)	2.6310(5)
Cm	2.5653(7)	2.5667(6)	CO	2.5875(7)	2.5882(6)
Dm	2.6115(8)	2.6102(6)	DO	2.6349(8)	2.6370(5)
BO-Cm	2.6612(9)	2.6650(5)	Bm-CO	2.6367(10)	2.6404(4)
Dm	2.6524(8)	2.6545(4)	DO	2.6428(8)	2.6423(4)
Cm-Dm	2.6533(9)	2.6550(6)	CO-DO	2.6884(9)	2.6889(6)

Anisotropic extinction was slightly more satisfactory than isotropic extinction. Refinement of split positions for Na was unsatisfactory, and refinement of anharmonic terms did not produce values significantly different from 0. Final values of $R(F^2)$ and $wR(F^2)$ are 0.0223 and 0.0298. The final difference-Fourier synthesis is essentially featureless. Tables 4–6 compare bond lengths and angles for low albite at room temperature (Harlow and Brown, 1980) and 13 K. Table 7[1] lists structure factors.

Table 5. O–T–O and T–O–T angles

O-T_1O-O		RT	13K	O-T_1m-O		RT	13K
A1	BO	102.91(5)	102.79(3)	A1	Bm	109.50(5)	109.55(2)
	CO	115.99(5)	116.37(3)		Cm	112.50(5)	112.26(2)
	DO	104.04(5)	103.48(2)		Dm	107.31(4)	107.26(2)
BO	CO	112.21(5)	112.06(3)	Bm	Cm	108.23(5)	108.26(2)
	DO	111.16(5)	111.21(3)		Dm	111.31(5)	111.36(2)
CO	DO	110.08(5)	110.43(3)	Cm	Dm	108.02(5)	108.18(3)
Average		109.40	109.39			109.48	109.48
O-T_2O-O		RT	13K	O-T_2m-O		RT	13K
A2	BO	111.15(5)	111.03(2)	A2	Bm	107.21(4)	107.33(2)
	Cm	104.23(4)	104.42(2)		CO	105.96(4)	105.95(2)
	Dm	107.06(4)	106.97(3)		DO	108.51(4)	108.54(3)
BO	Cm	112.06(5)	112.17(2)	Bm	CO	110.14(5)	110.29(2)
	Dm	111.60(5)	111.51(2)		DO	110.22(5)	110.07(2)
Cm	Dm	110.34(5)	110.40(2)	CO	DO	114.46(5)	114.34(2)
Average		109.42	109.42			109.42	109.42

T-O-T	RT	13K
1O A1 1m	141.45(5)	140.39(2)
2m A2 2O	130.08(4)	129.53(2)
1O BO 2O	139.66(5)	139.22(2)
1m Bm 2m	161.20(5)	161.82(2)
1O CO 2m	129.88(5)	129.30(3)
1m Cm 2O	135.85(5)	136.05(2)
1O DO 2m	133.95(5)	133.80(2)
1m Dm 2O	151.84(5)	151.87(2)
Average	140.49	140.25

Table 6. Na–O distances

Na-O	13K	RT[a]	RT[b]	RT[c]
A2	2.3606(5)	2.372(1)	2.369	2.377, 2.264
DO	2.4187(6)	2.437(1)	2.435	2.437, 2.354
BO	2.4382(6)	2.461(1)	2.454	2.449, 2.579
A1	2.5005(6)	2.537(1)	2.535	2.671, 2.526
A1	2.6140(7)	2.671(1)	2.669	2.515, 2.824
CO	2.9706(8)	2.961(1)	2.978	2.960, 3.179
Dm	2.9969(6)	2.996(2)	3.003	2.988, 3.279
Cm	3.2678(8)	3.266(1)		3.277, 2.932
Bm	3.4510(7)	3.465(2)		3.473, 3.222

[a]HB; [b]Wainwright in Smith (1974); [c]Wenk and Kroll (1984), split positions.

Results and discussion

The geometry of the crystal structure at 13 K of Amelia albite is generally consistent with those of low albites at ambient temperature (Harlow and Brown, 1980; Wenk and Kroll, 1984) and higher temperature (Winter et al., 1977) when account is taken of reduced thermal motion. Figure 1 is a stereoview down **a*** showing the twisting of the double-crankshaft chains, the position of the Na atom, and the anisotropic displacement ellipsoids at 13 K. Figure 2 shows the linkage of Na to the nine nearest oxygen atoms (cf. Smith, 1974, fig. 4–11; Winter et al., 1977, fig. 7).

To a first approximation, the B displacement parameters for the framework atoms decrease about threefold as the temperature of Amelia albite drops from ambient to 13 K, and there is no major change in the anisotropy and orientation of each displacement ellipsoid. The ellipsoids for the T atoms are weakly anisotropic at both temperatures (Table 2: R_3/R_1 = 1.17–1.30, RT; 1.18–1.32, 13 K). Those for most of the oxygen atoms are oblate with the shortest axis approximately parallel to the vector between the two adjacent T atoms; the anisotropy decreases upon cooling (Table 2: R_3/R_1 = 1.47–1.97, RT; 1.35–1.69, 13 K). Minor differences between oxygen atoms can be explained by bonding to the Na atom.

At 13 K, the distances from Na to the nine nearest framework oxygens fall into two distinct clusters (Fig. 3): 2.36–2.61 and >2.97 Å. The five nearest oxygen atoms (Fig. 2) form an irregular deltahedron composed of triangular faces. With increasing temperature, the gap between the clusters decreases and essentially disappears at 1243 K (Winter et al., 1977). This conclusion is independent of the systematic bias in bond lengths from the swinging-arm effect (Winter et al., 1977; Table 7). Although the

[1] To obtain a copy of Table 7, order document AM-86-300 from the Business Office, Mineralogical Society of America, 1625 I Street, N.W., Suite 414, Washington, D.C. 20006. Please remit $5.00 in advance for the microfiche.

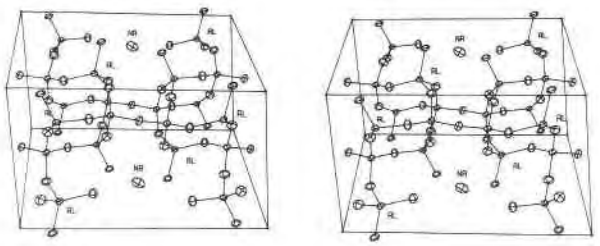

Fig. 1. Stereoplot of structure of low albite at 13 K. The **b** and **c** axes, respectively, point to the right and the top of the page, and the **a** axis tilts toward the reader. Ellipsoids at 99% probability.

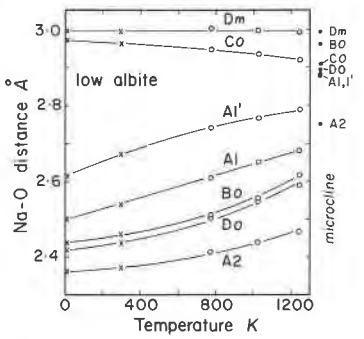

Fig. 3. Temperature variation of distances from Na to the seven nearest oxygen atoms in low albite. Cross: Amelia albite, Harlow and Brown (1980) and this paper; circle, Tiburon albite, Winter et al. (1977). The dots show K-O distances in low microcline at room temperature (Smith, 1974). Curves inserted by eye.

shorter Na–O distances increase considerably with temperature, they do not reach the K–O distances for microcline at room temperature (Fig. 3, dots).

The displacement ellipsoid of Na is more anisotropic than those of the framework atoms at elevated temperature, but at 13 K the distinction is smaller ($R_3/R_1 = 1.66$ (Na), 1.35–1.72 (oxygens), 1.18–1.32 (T)). The nine nearest oxygen atoms split into two opposing pairs of distant atoms and a cluster of five nearer ones, and the major displacement of Na is approximately in the directions of the distant oxygen atoms.

The above discussion reinforces the general conclusions already reached by earlier writers including Harlow and Brown (1980), Winter et al. (1977), Brown et al. (1984), and Kroll (1984), and further elaboration is unprofitable. Emphasis is now placed on the evidence for zero-point energy and on the complex relationship between T–O bond distances and stereochemical factors.

Zero-point motion

Earlier writers (e.g., Winter et al., 1977) concluded that the Na atom in low albite (but not in high albite) vibrates anisotropically about a single center-of-motion and does not jump between two centers-of-motion. This conclusion was based on a linear extrapolation of the experimental temperature factor B to zero at 0 K within error limits (e.g., Winter et al., 1977, figs. 5 and 6). The new data for 13 K confirm that B (Na) is linearly related to temperature, but there is a finite intercept of $B = 0.5$ Å^2 at 0 K (Fig. 4). Least-squares refinement of X-ray diffraction data may be complicated by the choice of atomic scattering factor (including the degree of ionization) and of models for absorption and extinction corrections. Refinement of neutron diffraction data is less sensitive to uncertainties since the absorption is negligible, and the scattering lengths are independent of the θ angle. The line for B(Na) in Figure 4 is firmly anchored by the two determinations for Amelia albite at 13 K and ambient temperature. The earlier X-ray data by Williams and Megaw (1964) and Quareni and Taylor (1971) were good enough to settle the question about the type of thermal motion, but inadequate for reliable extrapolation. Furthermore, it appears that the X-ray data for Tiburon albite at room temperature (Wainwright in Smith, 1974) may be biased with respect to neutron data for Amelia albite. Wenk and Kroll (1984, tables VIII and IX) have demonstrated the sensitivity of X-ray refinements of Cazadero albite to different assumptions.

Because the extrapolations for the T and O atoms (Fig. 4) also yield positive intercepts at 0 K, zero-point motion is the preferred cause rather than multiple centers-of-mo-

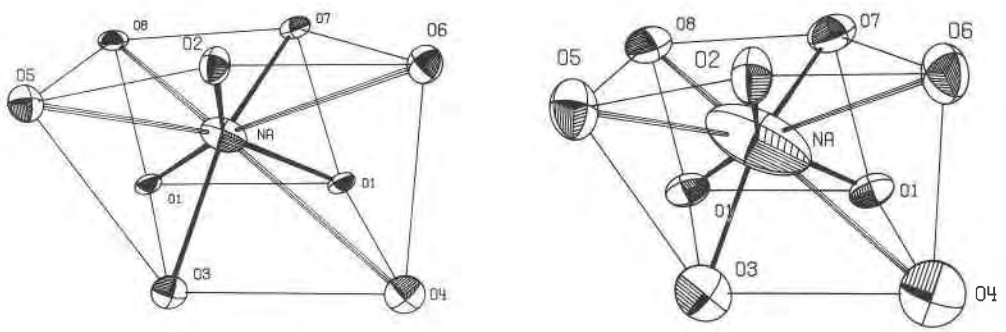

Fig. 2. Comparison of environment of Na atom (Fig. 1; lower position) at 13 K (left) and room temperature (right). Ellipsoids at 99% probability Oxygen atoms 1–8 are in sequence A1, A2 . . . D_m of Table 1. Linkages between Na and the five nearest oxygen atoms are accentuated.

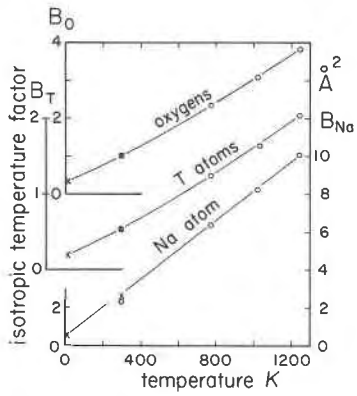

Fig. 4. Temperature variation of isotropic approximation of the thermal parameter (B in Å²) for Na, T, and oxygen atoms in low albite. Averages given for oxygen and T atoms. Curves inserted by eye. A straight line is given for Na, but a curved line would be expected for a Debye model. Symbols as in Figure 3.

tion. Similar B values to those in low albite at 13 K were obtained for natrolite and scolecite at about 20 K (Table 8), as expected for similar bond strengths in these framework structures and a common set of zero-point energies. Further structure determinations are needed before a quantitative explanation is attempted. In the meantime, the general relationships between the values in Table 8

Table 8. Apparent thermal parameters (isotropic approximation) at low temperature

Structure	Temperature (K)	B(Na)	B(Al)	B(Si)	B(Ca)
low albite[a]	13	0.56(1)	0.20(1)	0.19-0.20(1)	
natrolite[b]	20	0.52(1)	0.27(1)	0.27(1)	
scolecite[c]	20		0.19-0.20(2)	0.17-0.18(1)	0.24(2)

[a]this paper; [b]Artioli, Kvick and Smith (1984); [c]Kvick, Ståhl and Smith (1985)

are qualitatively plausible in relation to the atomic mass (e.g., Ca is twice as heavy as Na) and the force constants (e.g., values for low albite deduced from infrared and Raman spectra; von Stengel, 1977, table 3). Furthermore, the values in Table 8 are similar to measured B values at low temperature and to values for the zero-point energy parameter B_0 in simple high-symmetry structures listed in the *International Tables for X-ray Crystallography*, volume III, (MacGillavry and Rieck, 1962, tables 3.3.5.1A and D): Na in NaCl at 20 K, $B_0 = 0.60$ Å²; Al in Al metal, $B_0 = 0.27$ Å²; Si in Si metal, $B_0 = 0.16$ Å²; Ca in Ca metal, $B_0 = 0.32$ Å².

Stereochemical interpretation of T–O bond distances

Distances and angles obtained from low-temperature atomic coordinates are significantly more useful for sta-

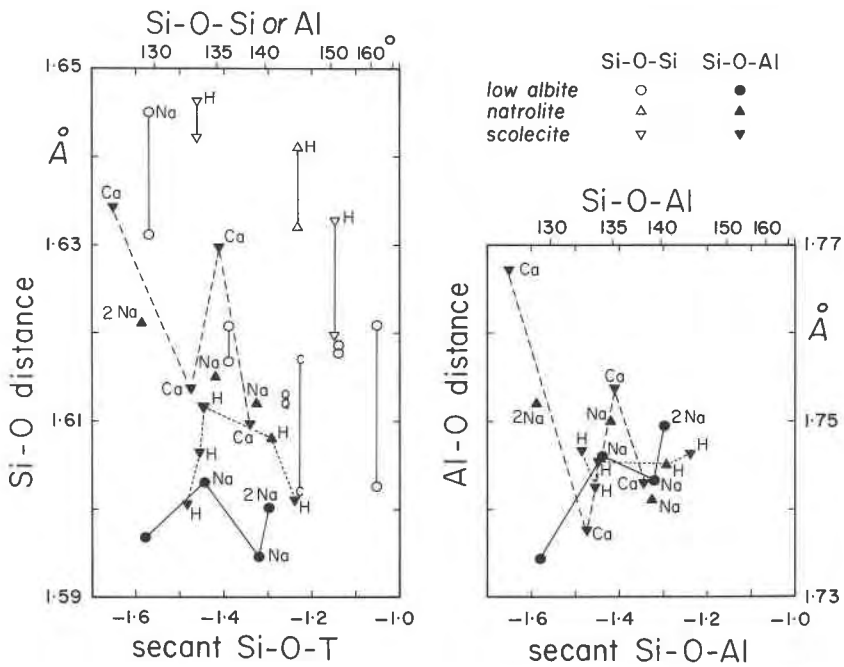

Fig. 5. Relation between secant Si–O–(Si or Al) and both Si–O . . . (Si or Al) and Al–O . . . Si in low albite (circle; 13 K; this paper), natrolite (upright triangle; 20 K; Artioli et al., 1984), scolecite (reversed triangle; 20 K; Kvick et al., 1985), cristobalite (C; 10 K; Pluth et al., 1984) and quartz (Q; 13 K; Lager et al., 1982). Pairs of open symbols (left) denote Si–O–Si. Each oxygen linked to Si and Al is represented by a filled symbol in the left and right drawings. H, Na, 2Na, and Ca denote extraframework ions bonded to the oxygens. Vertical lines (left-hand plot) join Si–O distances to the same oxygen. Long dashes join Si–O distances (left-hand plot) and Al–O distances (right-hand plot) to oxygens linked to 1 Ca in scolecite. Short dashes refer similarly to hydrogen-bonded oxygen. The continuous lines for albite link oxygens bonded to 0, 1, and 2 Na.

tistical analysis of the bond systems than data obtained at high temperature, insofar as the swinging-arm effect is minimized near zero kelvin. Figure 5 compares data for framework structures at 10–20 K, all of which have complete Si,Al order in tetrahedral sites. The zero-point motion should be similar for all these materials.

Tetrahedral distances in aluminosilicates have been interpreted using purely electrostatic ionic models (Baur, 1970, 1981), in terms of hybridization of tetrahedral or oxygen atom orbitals (Cruickshank, 1961; Brown and Gibbs, 1970) and in terms of molecular-orbital models (review in Newton, 1981; Gibbs, 1982; Geisinger et al., 1985). All models are actually related to each other. The ionic bond strength parameter (p_0) used by Baur and by others, and based on Pauling's rules for bonding in solids, can be interpreted in terms of molecular-orbital calculations (Burdett and McLarnan, 1984). Also the hybridization degree of the input atomic orbitals is an important factor influencing the directionality and the overlap populations of the localized molecular orbitals used to express the degree of bonding in aluminosilicate tetrahedra (Newton, 1981; Geisinger et al., 1985). The linear correlations between calculated bond-overlap populations (n(T–O)) and p_0 (Gibbs, 1982; Geisinger et al., 1985) can be attributed to either covalent or ionic models and do not resolve the still open problem of the degree of ionic character in tetrahedral bonds of aluminosilicates (Pauling, 1980; Stewart et al., 1980).

Variations in tetrahedral distances have been related to six factors: the Al content in the T site, the coordination number of the bridging oxygen, the type of adjacent T atom, the type of extraframework atoms and their distances from the oxygen, the variation of bridging T–O–T angles, and the variation of internal tetrahedral O–T–O angles.

The principal factor influencing the mean T–O length of a tetrahedron is the Al content (Ribbe et al., 1974), and many attempts have been made to deduce determinative curves (Smith, 1974; Ribbe, 1984). Individual T–O distances depend on all of the above factors. Although the control exerted on a bond length by the type of adjacent T atom is evident in Figure 5 (open vs. closed symbols in the left-hand diagram), other factors must have complex effects, producing a rather confused picture. A weak correlation between T–O distances and negative secant of (T–O–T) angle was reported for the aluminosilicate group (review in Gibbs, 1982) and for zeolites in particular (Artioli et al., 1984; Kvick et al., 1985). The negative secant of the angle at the bridging oxygen was used as a parameter modeling the bond-length variation because it reflects the degree of mixing of s- and p-type orbitals on the atom (Coulson, 1961; Newton and Gibbs, 1980; Newton, 1981). This correlation however appears to be rather weak for the minerals in Figure 5. Assuming perfect Si,Al ordering, the first-neighbor coordination of the oxygen atoms alone (shown by abbreviations near the symbols on Fig. 5) does not completely clarify the picture. Some of the discrepancies within each pair of Si–O distances to the same oxygen atom (0.018–0.001 Å) are greater than the sum of the individual experimental uncertainties of the bond lengths (0.003 Å). Only one of the longer bond lengths belongs to an oxygen coordinating a Na atom, and only some of the other long distances are to oxygen acceptors of weak hydrogen bonds. Just for low albite, the longer distance in each pair belongs to a Si atom having two Al and two Si atoms as tetrahedral neighbors. The shorter distance is for a Si atom surrounded by one Si and three Al tetrahedral atoms. This would indicate a small influence by the chemical content of second-neighbor tetrahedra on the geometry of the tetrahedron under examination. Also each oxygen, which is not associated with Na or H atoms, displays a smaller Si–O distance on average than oxygens bonded to Na or H. In each group there is at best only a weak negative correlation between Si–O and negative secant (Si–O–Si). No simple correlation exists for oxygens that have the same type of coordination, specifically those oxygens in scolecite that are bonded to Ca atoms (long dashed line) or to H atoms (short dashed line).

G. V. Gibbs kindly pointed out that for low albite there are good correlations between R(SiO) and f_s(Si) and between R(AlO) and f_s(Al) (nomenclature defined in Gibbs, 1982):

$$\mathrm{R(SiO)} = 1.905 - 1.167 f_s(\mathrm{Si})$$

and

$$\mathrm{R(AlO)} = 1.816 - 0.290 f_s(\mathrm{Al}).$$

Conclusions

The present study of low albite at 13 K extends the general conclusions obtained by Harlow and Brown (1980) and Winter et al. (1977) from measurements at and above room temperature: in particular, the Na atom at low temperature is strongly bonded to five out of the nine nearest oxygen atoms, and its displacement is well represented by a single ellipsoid elongated in the direction of the weakest bonding. However, the vibration ellipsoids of Na, Al, Si, and O are larger than for a simple extrapolation to zero at 0 K and are qualitatively consistent with the presence of zero-point energy. Systematic measurements of the Raman, infrared, and ^{23}Na nuclear magnetic resonance spectra of low albite down to low temperature should prove instructive; in particular, there should be greater mixing of framework and extraframework vibrational modes at lower temperatures because of the shorter distances from Na to the five nearest oxygen atoms. Stereochemical interpretation of the T–O bond distances in low albite, natrolite, scolecite, quartz, and cristobalite at 10–20 K demonstrates that consideration of first neighbors is not sufficient. Measurements of other important framework structures (including coesite) are in progress to provide thorough tests of stereochemical models.

Acknowledgments

This research was performed at Brookhaven National Laboratory under contract DE-AC02-76CH00016 with the U.S. De-

partment of Energy, Division of Chemical Sciences, Office of Basic Energy Sciences. It is part of a program on Disordered Materials supported by the Materials Research Laboratory at the University of Chicago funded by NSF Grant DMR 82-16892. GA is on leave of absence from the Università de Modena, Italia. We thank G. E. Harlow and G. E. Brown, Jr., for loan of the crystal, G. V. Gibbs for helpful analysis, and P. H. Ribbe for review of the manuscript.

References

Artioli, G., Smith, J.V., and Kvick, Å. (1984) Neutron diffraction study of natrolite, $Na_2Al_2Si_3O_{10}\cdot 2H_2O$, at 20 K. Acta Crystallographica, C40, 1658–1662.

Baur, W.H. (1970) Bond length variation and distorted coordination polyhedra in inorganic crystals. American Crystallographic Association Transactions, 6, 129–155.

——— (1981) Interatomic distance predictions for computer simulation of crystal structures. In M. O'Keefe and A. Navrotsky, Eds. Structure and bonding in crystals, volume II, 31–52. Academic Press, New York.

Becker, P., and Coppens, P. (1974) Extinction within the limit of validity of the Darwin transfer equation. I. General formalism from primary and secondary extinction and their application to spherical crystals. Acta Crystallographica, A30, 129–147.

Brown, G.E., and Gibbs, G.V. (1970) Stereochemistry and ordering in the tetrahedral portion of silicates. American Mineralogist, 55, 1587–1607.

Brown, W.L., Openshaw, R.E., McMillan, P.F., and Henderson, C.M.B. (1984) A review of the expansion behavior of alkali feldspars: Coupled variations in cell parameters and possible phase transitions. American Mineralogist, 69, 1058–1071.

Burdett, J.K., and McLarnan, T.J. (1984) An orbital interpretation of Pauling's rules. American Mineralogist, 69, 601–621.

Busing, W.R., and Levy, H.A. (1964) The effect of thermal motion on the estimation of bond lengths from diffraction measurements. Acta Crystallographica, 17, 142–146.

Catlow, C.R.A., and Mackrodt, W. D., Eds. (1982) Computer simulation of solids. Lecture Notes in Physics, no. 166. Springer, Berlin.

Coulson, C.A. (1961) Valence. Oxford University Press, London.

Cruickshank, D.W.J. (1961) The role of 3*d*-orbitals in π-bonds between (a) silicon, phosphorus, sulfur, or chlorine and (b) oxygen or nitrogen. Journal of the Chemical Society, 1961, 5486–5504.

Ferguson, R.B., Traill, R.J., and Taylor, W.H. (1958) The crystal structures of low-temperature and high-temperature albites. Acta Crystallographica, 11, 331–348.

Geisinger, K.L., Gibbs, G.V., and Navrotsky, A. (1985) A molecular orbital study of bond length and angle variations in framework structures. Physics and Chemistry of Minerals, 11, 266–283.

Gibbs, G.V. (1982) Molecules as models for bonding in silicates. American Mineralogist, 67, 421–450.

Harlow, G.E., and Brown, G.E., Jr. (1980) Low albite: An X-ray and neutron diffraction study. American Mineralogist, 65, 986–995.

Koester, L., Rauch, H., Herkens, M., and Schröder, K. (1981) Kernforschungsanlage Report JÜL-1755.

Kroll, H. (1984) Thermal expansion of alkali feldspars. NATO ASI Series. Series C, 137, 163–205. Reidel, Dordrecht, Netherlands.

Kvick, Å., Ståhl, K., and Smith, J.V. (1985) A neutron diffraction study of the bonding of zeolitic water in scolecite at 20K. Zeitschrift für Kristallographie, 171, 141–154.

Lager, G.A., Jorgensen, J.D., and Rotella, F.J. (1982) Crystal structure and thermal expansion of α-quartz SiO_2 at low temperature. Journal of Applied Physics, 53, 6751–6757.

MacGillavry, C.H., and Rieck, G.D., Eds. (1962) International tables for X-ray crystallography, volume III. Kynoch Press, Birmingham, England.

Newton, M.D. (1981) Theoretical probes of bonding in the disiloxy group. In M. O'Keeffe and A. Navrotsky, Eds. Structure and bonding in crystals, volume II, 175–193. Academic Press, New York.

Newton, M.D., and Gibbs, G.V. (1980) Calculated geometries and charge distributions for H_4SiO_4 and $H_6Si_2O_7$ compared with experimental values for silicates and siloxanes. Physics and Chemistry of Minerals, 6, 221–246.

Pauling, L. (1980) The nature of silicon-oxygen bonds. American Mineralogist, 65, 321–323.

Pluth, J.J., Smith, J.V., and Faber, J., Jr. (1985) Crystal structure of low cristobalite at 10, 293 and 473 K: Variation of framework geometry with temperature. Journal of Applied Physics, 57, 1045–1049.

Prewitt, C. T., Sueno, S., and Papike, J.J. (1976) The crystal structures of high albite and monalbite at high temperature. American Mineralogist, 61, 1213–1225.

Quareni, S., and Taylor, W.H. (1971) Anisotropy of the sodium atom in low albite. Acta Crystallographica, B27, 281–285.

Ribbe, P.H. (1984) Average structures of alkali and plagioclase feldspars: Systematics and applications. NATO ASI Series, Series C, 137, 1–54.

Ribbe, P.H., Megaw, H.D., Taylor, W.H., Ferguson, R.B., and Traill, R.J. (1969) The albite structures. Acta Crystallographica, B27, 1503–1518.

Ribbe, P.H., Phillips, M.W., and Gibbs G.V. (1974) Tetrahedral bond length variations in feldspars. In W.S. MacKenzie and J. Zussman, Eds. The feldspars, 25–48. Manchester University Press, Manchester, England.

Smith, J.V. (1974) Feldspar minerals, volume 1. Springer, Berlin.

Stewart, R.F., Whitehead, M.A., and Donnay, G. (1980) The ionicity of the Si–O bond in low-quartz. American Mineralogist, 65, 324–326.

von Stengel, M.O. (1977) Normal Schwingungen von Alkalifeldspäten. Zeitschrift für Kristallographie, 146, 1–18.

Wenk, H.-R., and Kroll, H. (1984) Analysis of $P\bar{1}$, $I\bar{1}$ and $C\bar{1}$ plagioclase structures. Bulletin de Minéralogie, 107, 467–487.

Williams, P.P., and Megaw, H.D. (1964) The crystal structures of low and high albites at −180°C. Acta Crystallographica, 17, 882–890.

Winter, J.K., Ghose, S., and Okamura, F.P. (1977) A high-temperature study of the thermal expansion and the anisotropy of the sodium atom in low albite. American Mineralogist, 62, 921–931.

Winter, J.K., Okamura, F.P., and Ghose, S. (1979) A high-temperature structural study of high albite, monalbite, and the analbite-monalbite phase transition. American Mineralogist, 64, 409–423.

Manuscript received June 7, 1985
Manuscript accepted January 17, 1986